euspen's 26th International Conference & Exhibition, Krakow, PL, June 2026
www.euspen.eu

Autocollimation and Reflected-Power Optimization in High-Refractive-Index Glass Retroreflectors for Robust, Cost-Effective Systems

Mateusz Sosin[1], Martin Dušek[1,2], Jean-Christophe Gayde[1], Kryštof Polák[1,2], Miroslav Šulc[2,3], Leonard Watrelot[1]

[1]*CERN – European Organization for Nuclear Research, Geneva, Switzerland*
[2]*Technical University of Liberec, Liberec, Czech Republic*
[3]*Institute of Plasma Physics of the Czech Academy of Sciences, Prague, Czech Republic*

Mateusz.sosin@cern.ch

Abstract

Spherical ball lenses with a refractive index of about 2 have, for several years, been recognized as a cost-effective alternative to classical mirror retroreflectors, owing to their ability to reflect incident light back toward its source with near-perfect fidelity. Their functionality, however, extends beyond basic retroreflection. When a substantial part of the ball is illuminated with coherent input, such as Gaussian beams, the reflected light forms so-called Structured Laser Beams (SLBs)—pseudo-non-diffractive optical beams. These beams arise from the interference of reflected light, with specific phase delays imposed on the coherent input by optical aberrations within the high-refractive-index glass sphere. This mechanism generates beams with a bright central core surrounded by concentric rings, capable of maintaining their spatial structure over theoretically unlimited propagation distances. SLBs exhibit an exceptionally low divergence of the inner core (down to approximately 10 µrad). When produced using glass-balls placed in the path of a divergent Gaussian beam with a spherical wavefront, the part of the light that enters the ball is reflected as an SLB, demonstrating excellent autocollimation, making such a reflector highly attractive for simple, cost-effective metrological systems. This paper outlines the operational principles, describes a qualitative measurement campaign using CERN's FSI systems while demonstrating reflected intensity optimization via ball diameter selection for robust autocollimation.

Keywords: metrology, interferometry, optical, high-refractive-index glass ball retroreflector

1. Introduction

High–refractive–index glass spheres (with n ≈ 2) have recently emerged as an attractive, low–cost alternative to classical mirror-based retroreflectors in optical metrology. Their usefulness was initially attributed to the simple geometric mechanism of refraction and internal reflection inside a homogeneous sphere [1-4], which enables light to return close to its incident direction over exceptionally large acceptance angles -up to 360° in principle - as demonstrated for S-LAH79 glass spheres with n = 1.996 at 633 nm [1]. Such "ball retroreflectors" have already been implemented in alignment and interferometric systems where compact, robust, and omnidirectional optical targets are required [1-3, 5].

However, the optical behaviour of these elements extends far beyond basic retroreflection. Due to the perfect rotational symmetry of the sphere and the large refractive volume traversed by the incoming radiation, ray optics is not sufficient for the description of the emerging field. When a coherent Gaussian beam illuminates a sufficiently large fraction of the spherical surface, rays travelling through different radial zones acquire different optical path lengths. This introduces controlled phase delays that are rotationally symmetric, dominated by spherical aberrations and by the defocus aberration. As shown in [6, 7], the resulting interference field forms a structured output beam with transverse intensity resembling a Bessel-type distribution (cf. Fig.1a).

This beam, referred to as a Structured Laser Beam (SLB), exhibits a bright, narrow central core surrounded by concentric rings [7]. SLBs belong to the class of pseudo–non-diffractive beams: their inner core maintains low divergence, typically of order 10 µrad, over propagation distances reaching hundreds of meters. Experimental results have shown SLB propagation over 140 m with a preserved millimetre-scale core diameter [7], and successful propagation has been demonstrated up to 900 m [8]. This behaviour distinguishes SLBs from Gaussian beams, which diverge significantly under comparable conditions.

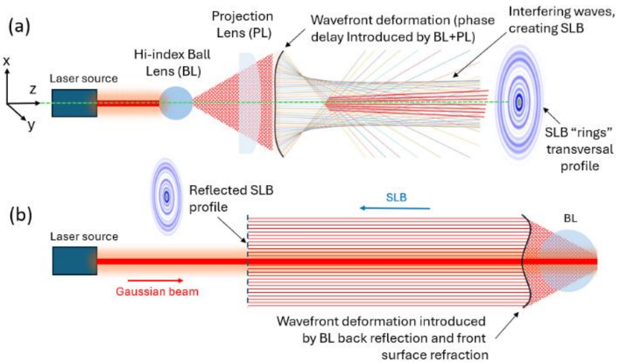

Figure 1. Schematic of two SLB generation methods: (a) wavefront shaping via projection through a high-index ball lens (BL) and a projection lens (PL); (b) wavefront shaping via back-surface reflection and front-surface refraction in the high-index BL.

A particularly relevant configuration for interferometric measurements arises when a high-index glass ball is used not as a forward generator of SLBs (cf. Fig.1a), but as a *retro-reflector* *that sends a structured beam back toward the source*. This special case is explicitly described in [6], where the spherical ball lens both returns the beam and imposes the aberration-driven phase structure responsible for SLB formation (cf. Fig.1b). When a Gaussian beam is reflected by the glass reflector, the portion of light entering the ball is returned, forming a back-reflected SLB. Such a configuration produces a stable, autocollimating return beam, with a high-intensity SLB central core, without requiring complex optical assemblies.

This makes high-index glass balls particularly appealing for robust, cost-effective implementations of these reflectors within interferometric systems.

The objective of this initial study is to qualitatively validate SLB formation and power integration in high-index glass retroreflectors via lab experiments, comparing trends to wave optical models without full quantitative calibration.

2. Enhancing optical system performance through high-index glass ball reflector properties

Two properties of high-refractive-index glass ball reflectors (with n ≈ 2) are particularly relevant for interferometric distance measurement architectures: (1) their ability to generate an autocollimated, high-intensity Structured Laser Beam (SLB) core upon reflection, and (2) the possibility of optimizing the reflected SLB core power by appropriately selecting the reflector diameter. Together, these properties enable simple, alignment-tolerant, and power-scalable optical layouts that are especially attractive for fibre-based measurement systems.

The autocollimation effect greatly simplifies the optical head design in interferometric systems (eg. using bare fibre simplified optics). When the measurement beam is launched directly from a bare optical fibre, the emitted wavefront is approximately spherical, and the beam acquires a conical shape determined by the fibre's Numerical Aperture (NA). Upon interacting with the high-index spherical reflector, the SLB-forming mechanism causes the bright central core of the reflected field to propagate back along the axis of the incoming spherical wavefront—effectively steering the main energy concentration back toward the fibre tip (cf. Fig. 2).

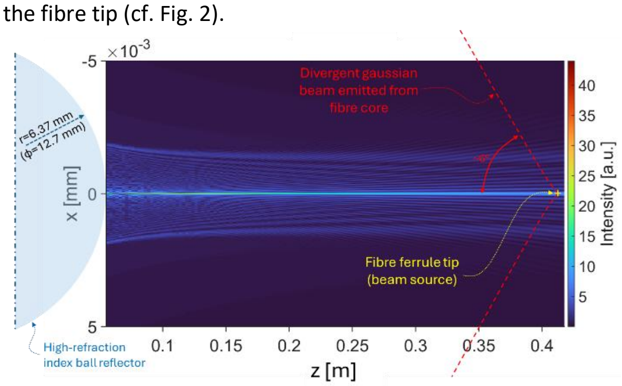

Figure 2. Longitudinal profile of the SLB field amplitude, created as back reflection from ϕ12.7 mm TAFD 55 glass ball reflector (at incident Gaussian beam of λ = 1550 nm), obtained from numerical simulations.

As a result, even with minimal or no collimating optics, a significant portion of the reflected SLB core is efficiently coupled back into the small fibre aperture. Simulations (as illustrated in Fig. 2) demonstrate that the bright central core remains narrow and well confined, enabling stable and robust power return even under relaxed alignment conditions. This geometry is therefore highly advantageous for compact interferometric distance sensors, where optical simplicity, coupling robustness, and compactness are essential.

In addition to its autocollimation capability, the high-index glass ball reflector enables direct control over the SLB core power by tailoring its diameter. In the considered configuration, the ball is illuminated by a Gaussian beam, and the reflected field assumes an SLB-like transverse structure. This transverse intensity distribution can be approximated by:

$$I_{SLB(x,y)} \approx I_0(J_0\,(k_T \cdot r))^2, \quad r = \sqrt{(x - x^0)^2 + (y - y^0)^2}, \tag{1}$$

were, J_0 is the zeroth-order Bessel function of the first kind, I_0 is the peak on-axis intensity of the SLB core, and k_T is the transverse wave-vector determined by the SLB generator [9], x-y coordinates as on Fig. 1. For a fixed SLB configuration, the radius of the SLB core (defined by the first dark ring of the Bessel pattern) is essentially independent of the diameter D of the high-index glass ball.

When the ball is illuminated by a Gaussian beam with $1/e^2$ radius w (for simplicity we assume the axis of the Gaussian beam concentric with ball lens centre), the optical power intercepted by the ball aperture (diameter D) is:

$$P_{in}(D) = \left(\frac{\pi I_{G0} w^2}{2}\right) \cdot \left[1 - \exp\left(-\frac{D^2}{2w^2}\right)\right], \tag{2}$$

where I_{G0} is the peak intensity of the incident Gaussian beam. A fixed fraction η_{core} of this power forms the SLB-like central core after reflection. Thus:

$$P_{core}(D) \approx \eta_{core} \cdot P_{in}(D), \tag{3}$$

and the core intensity:

$$I_{core}(D) \approx \frac{P_{core}(D)}{\pi \cdot r_{core}^2}. \tag{4}$$

For ball diameters considerably smaller than the incident Gaussian beam width ($D \ll w$), the intercepted power—and therefore both $P_{core}(D)$ and $I_{core}(D)$ —scales approximately with D^2. In this regime, increasing the reflector diameter effectively integrates a larger portion of the Gaussian beam power, which is subsequently funneled into the same narrow SLB core. Consequently, the SLB core intensity grows with the illuminated area of the reflector. For large diameters ($D \gg w$), the intercepted power saturates as the reflector already captures nearly all of the Gaussian beam energy; further increases in D no longer raise the SLB core intensity.

This behaviour provides a simple and effective optimization parameter: by selecting the reflector diameter, the designer can scale the SLB core power. Such power-scaling capability offers additional flexibility for adapting the returned optical signal level to detector sensitivity, interferometer dynamic range, or long-distance propagation requirements.

High–refractive–index glass ball reflectors have been widely investigated to be used within CERN's Frequency-Sweeping Interferometry (FSI) systems since almost a decade [3], primarily as compact, omnidirectional retroreflectors enabling robust position monitoring with minimal optical hardware [5]. In their earliest implementations, these elements were treated as simple reflective targets: the design philosophy intentionally favoured cost-effective instrumentation composed only of a fibre-ferrule launch and a spherical reflector. Nevertheless, operational experience accumulated across large-scale installations consistently revealed two favourable characteristics: (i) a high return power, and (ii) a clean and stable interferometric signal response.

These empirical observations, together with the parallel development of SLB theory and experiments [6–9], triggered an investigation into the power-integration behaviour and autocollimation properties of high-index ball reflectors, described hereafter.

3. Qualitative measurements campaign

The aim of the measurement campaign presented in this section is to provide an initial qualitative study, establishing visual and trend agreement between experiment and wave optical SLB models. Two complementary investigations were performed: (i) a quantitative assessment of reflected signal magnitude as a function of reflector diameter, and (ii) a direct visualisation of the generated SLB core to confirm its spatial structure.

3.1. Diameter-dependent reflected power measurements

To assess the influence of reflector diameter on the returned signal level, six commercial high-index glass ball reflectors (Hoya TAFD-55 and Schott P-SF68, uncoated, nominal refractive index *n* ≈ 2; see Fig. 3) with diameters of 4 mm, 6 mm, 10 mm, 12.6 mm, 12.7 mm, and 30 mm were examined. Each reflector was mounted on the same conical support and tested at two axial distances from a bare-fibre Gaussian-beam launch: 0.42 m and 1.1 m.

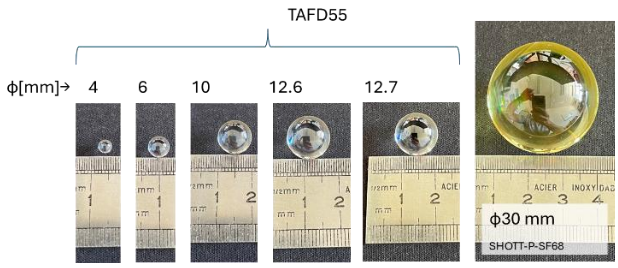

Figure 3. Measured glass ball reflectors.

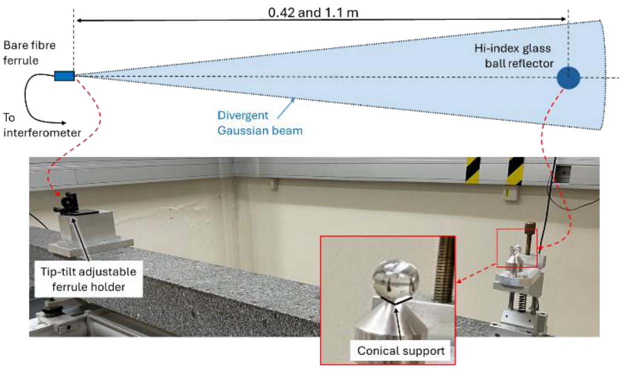

Figure 4. Measurement setup - bare fibre–ferrule installed in the tip–tilt mount to align the output Gaussian beam axis concentrically with the reflector.

The input beam was coarsely aligned so that the maximum-intensity region of the spherical Gaussian beam was positioned approximately 1 cm above the conical support—placing it close to the geometric centre of the reflectors (see Fig. 4). No additional collimation optics were employed, in order to replicate the simple, minimal-hardware configurations typical of FSI installations, with Gaussian beam encompassing the reflector.

For each ball diameter and distance, 21 independent measurements were acquired using CERN's FSI interferometer [5]. The system simultaneously recorded the reconstructed optical distance and the magnitude of the interferometric response, received through the aperture of the fibre. Although the measured magnitude does not represent an absolute optical power—because the FSI amplitude is not calibrated to physical intensity—it provides a consistent and reliable relative indicator of the returned power under fixed operating conditions. Throughout all tests, the optical power emitted from the fibre-ferrule launch (sweeping over the C-band, ~1530–1565 nm) was kept constant at approximately 5 mW. The resulting signal magnitudes as a function of ball diameter are summarised in Fig. 5.

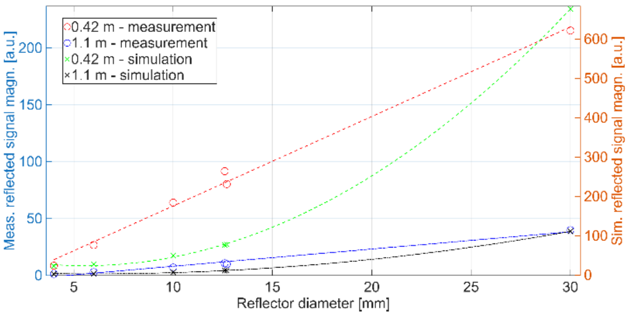

Figure 5. Comparison of measured and simulated (reflected) power for different ball reflectors.

In parallel, numerical simulations were carried out using an SLB propagation model based on the framework presented in [9]. For each reflector diameter, the model computed the expected SLB core intensity—under equivalent Gaussian illumination—and the fraction re-coupled back into the fibre ferrule (see Fig. 2). The resulting simulated trend is plotted alongside the measurements in Fig. 5 for comparison.

The experimental data show that the measured interferometric magnitude increases approximately linearly with reflector diameter, in contrast to the quadratic (D^2) dependence predicted by the simulation. In the theoretical model, the D^2 scaling arises because larger spheres intercept a proportionally greater fraction of the Gaussian beam, while the resulting SLB core maintains an approximately diameter-independent width. The observed linear trend can be explained by several practical factors. First, residual alignment errors: maintaining perfect coaxiality between the Gaussian beam and each sphere was challenging due to the single-reflector mounting approach. Even small lateral misalignments, introduced when swapping reflectors, modify the fraction of Gaussian power incident on the effective aperture of the sphere, thereby altering the returned SLB core power. Second, diameter-dependent variations in coupling efficiency may also play a role; SLB cores produced by spheres of different sizes might couple into the detection optics with slightly different efficiencies, though quantifying this effect lies beyond the scope of the present study. Third, the largest sphere tested (ϕ30 mm, SCHOTT P-SF68) was fabricated from a different glass than the smaller ones (HOYA TAFD55). The corresponding differences in refractive index and material properties could influence internal attenuation and Fresnel losses, contributing to the deviation from the idealised D^2 trend.

Despite these limitations, the overall increase in returned power with reflector diameter is clearly evident, qualitatively confirming the expected power-integration behaviour of high-index spheres. This monotonic trend validates diameter as an optimization parameter for practical FSI systems.

3.2. Direct visualisation of the SLB core

To confirm the formation of SLB with high intensity core under reflective illumination, a second experiment was conducted. In this setup, illustrated in Fig. 6, a fibre-ferrule emitter launched a divergent Gaussian beam toward a partially reflective mirror, which redirected a portion of the light toward a ϕ12.7 mm glass ball reflector. The reflector generated a retroreflected SLB that subsequently passed back through the semi-reflective mirror and a beam expander—used to scale the SLB to the size of the camera's CCD—and was finally imaged onto a near-infrared-sensitive camera (Gentec BEAMAGE-4M-IR series). This configuration enabled direct observation of both the intensity distribution and spatial structure of the resulting SLB.

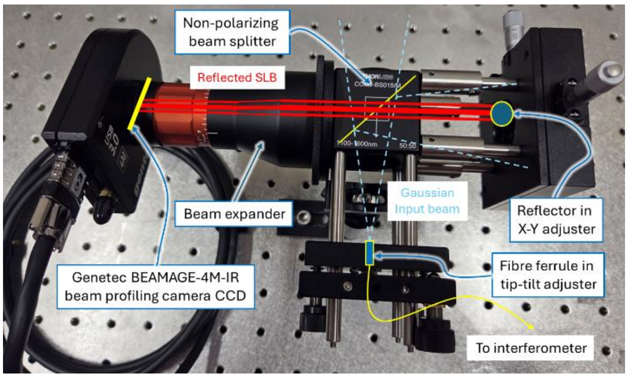

Figure 6. Measurement setup to visualize the reflected SLB and intensity of the core.

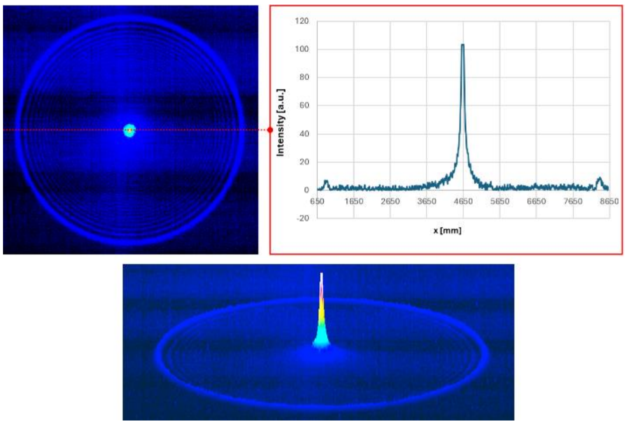

Figure 7. Visualization of the measurement of the SLB pattern with a clearly defined high-intensity core.

The recorded intensity distribution is shown in Fig. 7. The image reveals the characteristic SLB morphology [7,8]: a bright, narrow central core—with a width far below that of the incident Gaussian beam—surrounded by well-defined concentric rings of decreasing intensity. The clear separation between the high-intensity core and its surrounding rings confirms the expected quasi-Bessel, pseudo-non-diffractive structure. Most importantly for optimization of optical applications, the central core is smooth, symmetric, and sharply confined, indicating that a substantial fraction of the power is concentrated into a spatial mode that can be efficiently coupled back into the small acceptance aperture of a fibre or compact photodetector.

This observation provides direct, visual confirmation of the SLB-based retroreflection mechanism responsible for the strong and stable return signals seen in operational FSI systems.

4. Conclusions

The measurement campaign provides qualitative confirmation that high-index glass ball retroreflectors are capable of integrating a substantial fraction of the incident optical power and returning it as a structured, autocollimated beam. Crucially, the paper demonstrates that this behaviour cannot be fully understood using ray optics alone. By incorporating the wave nature of light into the analysis, we are able to model the formation and propagation of the SLB, including features such as the intensity structure, core narrowing, and coupling efficiency—effects that arise beyond purely geometric descriptions.

Although the expected D^2 scaling of the SLB core power was not fully reproduced experimentally—most likely due to coupling-efficiency limits, alignment imperfections and biggest reflector material difference—the monotonic increase of the returned signal with reflector diameter reinforces the underlying power-integration principle predicted by wave-optical model.

Direct imaging of the reflected field further confirms the emergence of a narrow, high-intensity SLB core, well suited for coupling into compact optical launches such as bare fibre ferrules. This provides experimental validation that ball-based retroreflectors can serve as efficient, alignment-tolerant elements in interferometric systems when both ray- and wave-optical effects are properly accounted for.

The results presented here represent an initial exploration aimed at establishing qualitative agreement between experiment and wave-enhanced modelling of SLB behaviour. A more comprehensive quantitative study—including calibrated power measurements, angular-tolerance characterisation, detailed wavefront analysis, and long-distance propagation tests—will be reported in future work.

References

[1] M. Sulc, "High index glass spherical targets for laser interferometry," ser. 1-st PACMAN Workshop. Geneva, Switzerland: CERN, February 2015. [Online]. Available: https://indico.cern.ch/event/332431/contributions/775845.

[2] G. Kautzmann, J.-C. Gayde, F. Klumb, Y. Kadi, J. Bensinger, K. Hashemi, and M. Sulc, "HIE Isolde – General Presentation of MATHILDE," CERN, Geneva, Tech. Rep., 2014. [Online]. Available: https://cds.cern.ch/record/2040166.

[3] S. W. Kamugasa, "Development and validation of a Frequency Scanning Interferometry Network for Compact Linear Collider component fiducialization," Ph.D. dissertation, ETH Zurich, 2018. [Online]. Available: https://doi.org/10.3929/ethz-b-000317637.

[4] Egidi, A.; Balsamo, A.; Pisani, M. High-Index Glass Ball Retroreflectors for Measuring Lateral Positions. Sensors 2019, 19, 1082. https://doi.org/10.3390/s19051082

[5] M. Sosin; J.D. Gonzalez Cobas; M. Isa; R. Leach; M. Lipiński; V. Rude; J. Rutkowski; L. Watrelot. An Interferometric Multi-Sensor Absolute Distance Measurement System for Use in Harsh Environments. Sensors 2025, 25, 5487. Available: https://doi.org/10.3390/s25175487

[6] M. Sulc and J.-C. Gayde, "An optical system for producing a Structured Beam," Patent EP3564734, 2019. [Online]. Available: https://data.epo.org/publication-server/rest/v1.2/patents/EP3564734NWA1/document.html.

[7] J.-C. Gayde, M. Sulc, and K. Polak, "Introduction to structured laser beam for alignment and status of the r&d," in 16th International Workshop on Accelerator Alignment (IWAA 2022). Ferney Voltaire (France). CERN Document Server, https://cds.cern.ch/record/2849065/, October 2022.

[8] Gayde, J.-C., et.al. The potential contribution of a structured laser beam to accelerator alignment technology. In Proceedings of the 14th International Particle Accelerator Conference (IPAC'23) (pp. 4044–4046). Venice, Italy: JACoW Publishing. https://doi.org/10.18429/JACoW-IPAC2023-THPA041.

[9] K. Polak, M. Sulc, and J.-C. Gayde, "Structured laser beam in non-homogeneous environment," in 16th International Workshop on Accelerator Alignment (IWAA 2022). Ferney Voltaire (France): CERN Document Server, https://cds.cern.ch/record/2849070, October 2022.